Journal of Superconductivity and Novel Magnetism (2018) 31:3509–3514
https://doi.org/10.1007/s10948-018-4735-3

ORIGINAL PAPER

Production Procedure and Characterization of Zn-Doped Y-123 Superconducting Samples Prepared by Sol-Gel Method

E. Asikuzun[1,2]

Received: 29 January 2018 / Accepted: 14 May 2018 / Published online: 25 May 2018

Abstract

The superconducting $YBa_2Cu_{3-x}Zn_xO_7$ (Y-123) bulk materials have been synthesized by using the sol-gel method. Samples are produced as undoped Y-123 and transition metal (Zn)-doped Y-123. Before the final heat treatment, the samples are calcined at 850 °C for 24 h. This process is repeated three times. Then, samples are sintered at 950 °C for 24 h in an air environment and at 500 °C for 5 h in an oxygen atmosphere. The synthesized products are characterized by XRD, R-T, and Vickers microhardness tester. The XRD investigation revealed that the prepared sample has an orthorhombic structure. According to XRD measurements, an orthorhombic structure has not changed with Zn doping. It was observed that undoped and Zn-doped samples have superconductivity properties by electrical measurements. T_c^{onset} is 89 K for undoped Y-123 sample, and the T_c^{onset} value decreases monotically with Zn addition. All samples show metallic behavior above T_c^{onset} temperature. As a result of Vickers microhardness measurements, it is observed that all samples have reverse indentation size effect (RISE) behavior.

Keywords Sol-gel · Superconductivity · Zn · Vickers microhardness

1 Introduction

The YBCO superconductor discovered by Wu in 1987 has a transition temperature above 77 K [1]. The most of superconducting materials were investigated by a low critical temperature close to a liquid helium temperature of 4.2 K before 1987. In technological high-temperature superconducting cuprates with high T_c based on lanthanides, barium copper oxides were discovered and found useful for industrial applications. The structure contains a layer of yttrium atoms sandwiched between copper oxide planes, followed by a barium oxide layer, copper oxide chain, and another barium oxide layer. The oxygen content in YBCO determines the crystallographic structure and the hole concentration in the CuO_2 planes. For an oxygen content $x = 6$ (where $7 - \delta$), the compound YBCO is in the tetragonal and an insulator. Increasing the oxygen content up to $x = 6.6$, the compound undergoes a phase transition from tetragonal to orthorhombic [2–4].

It is seen that crystal formation is in the form of square plane and chain plane [1]. Production of pure and single phase is easy. Crystallographically, it is more uniform than other superconductors. Crystallographically, it is more uniform than other superconductors.

In this yttrium-based system, while charge carriers are holes and electrons above the critical temperature, charge carriers are electrons under the critical temperature. The YBCO system can be found in orthorhombic or tetragonal structure. YBCO has an orthorhombic room-temperature phase with cell parameters $a = 3.828$ Å, $b = 3.888$ Å, and $c = 11.65$ Å. The tetragonal phase is only observed at high temperature in a range between 750 and 900 °C. When decreasing the temperature and increasing the oxygen content of the sample, phase transition occurs at about 700 °C from the tetragonal to the orthorhombic phase. Many approaches have been tried for practical devices based on $YBa_2Cu_3O_{7-\delta}$ (YBCO) which is the only material for developing the high-T_c electronics [5].

It is structurally sensitive to the amount of oxygen. When heat treatment is performed in an oxygen environment, the structure forms in the $YBa_2Cu_3O_{7-\delta}$ form

✉ E. Asikuzun
easikuzun@kastamonu.edu.tr

[1] Faculty of Engineering and Architecture, Department of Metallurgy and Material Engineering, Kastamonu University, 37100 Kastamonu, Turkey

[2] Research and Application Center, Kastamonu University, 37100 Kastamonu, Turkey

and is superconducting. When it is heat treated in an oxygen-free or deficient amount of oxygen environment, tetragonal structure and the non-superconducting phase are obtained.

There are many test methods used to determine the mechanical properties of materials. The most common static load test methods are the tensile, compression, torsion, bending, hardness, and creep tests. The most common dynamic load test methods are the fatigue test and notch impact test [6–9]. Mechanical properties vary according to the type of applied load. Generally, there are two different load types as static and dynamic. The various mechanical properties of materials are determined depending on the load type applied. For example, fatigue toughness is one of important properties of the materials and is identified by the behavior of the material under applied dynamic load. Other material properties such as tensile strength, yield strength, fracture toughness, toughness, ductility, elastic modulus, and hardness are determined by the behavior of the material under applied static load [10–12].

The aim of this study is investigation of micromechanical and microstructural properties of materials. The X-ray diffraction (XRD) and Vickers microhardness measurements were performed to determine the structural properties and micromechanic properties of materials, respectively. In addition, electrical resistivity measurements are used to determine the superconductivity properties. These measurements and obtained results are given in Section 3.

2 Production Parameters and Analyses of Samples

In this study, all nano bulk materials are produced via the sol-gel method which, depending on production technique, includes ceramic, glass, and composite materials. To produce Zn-doped Y-123 samples, zinc acetate dihydrate powder is added at 0.01, 0.03, 0.1, and 0.3% ratios. For solutions, zinc acetate dihydrate, yttrium(III) acetate hydrate, barium acetate, and copper(II) acetate are used as precursors. Methanol and acetic acid are used as a solvent in preparing a homogenous solution. After weighing at appropriate rates, the precursors and solvents are stirred using the heater magnetic stirrer at 60 °C for 12 h12 h until a transparent solution is obtained. Then, $YBa_2Cu_{3-x}Zn_xO_7$ ($x = 0.01$, 0.03, 0.1, and 0.3) solutions are preheated at 300 °C for 30 min in air and are grounded. Grounded nanoparticles are pressed under 4 tons for 5 min into disk-shaped compacts with thicknesses of 2 mm and diameters of 10 mm. Pressed samples are calcined at 850 °C for 24 h. This process is repeated three times. Then, samples are sintered at 950 °C for 24 h, and while the furnace is cooled, an oxygen gas is supplied to samples at 500 °C for 5 h.

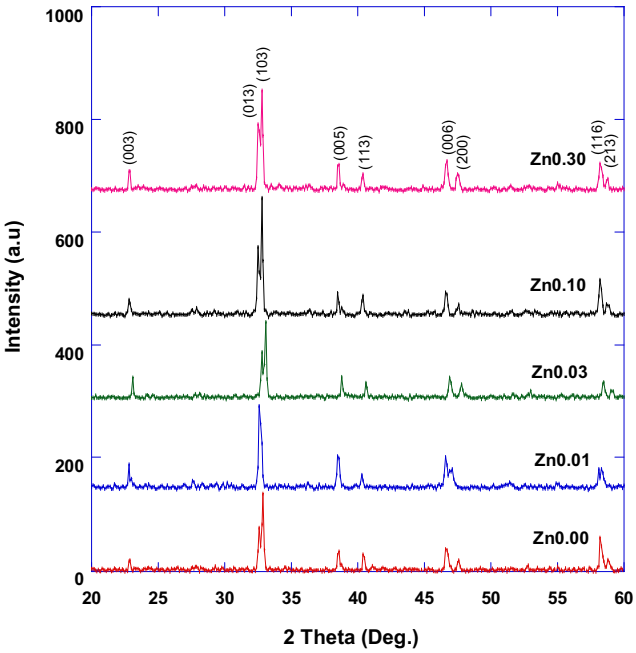

Fig. 1 XRD patterns of Zn-doped Y-123 nano bulk samples

The samples are named as $Zn_{0.0}$, $Zn_{0.01}$, $Zn_{0.03}$, $Zn_{0.10}$, and $Zn_{0.30}$ in other sections.

3 Result and Discussion

3.1 XRD Analyses of Superconducting Nanoparticles

X-ray diffraction measurements are performed by a Bruker D8 Advance X-ray powder diffractometer device using CuK_α radiation source ($\lambda = 0.154$ nm). Scanning rate and scan speed were $3° \leq 2\theta \leq 90°$ and 2° /min, respectively.

Figure 1 shows the XRD pattern of Zn-doped Y-123 bulk samples. Indexing of the pattern shows that all the samples are in orthorhombic structure and at the same peak at the same angle as undoped Y-123. It is also observed that the structure has not changed even after doping Zn. The symmetry has also not changed after doping. There is no phase of the Zn ions. This means that Zn^{2+} ions are replaced with Cu^{2+} ions in the YBCO lattice. It concludes that the addition of ZnO to pure YBCO has no significant effect on the structure and symmetry of the composites. The lattice parameters and grain size calculated by the Warren-Scherer formula [13] are listed in Table 1.

While the lattice parameters b and c decrease with Zn doping, the lattice parameter a increases with doping. The orthorhombic structure has not changed [14, 15]. As shown in Table 1, Zn-doped bulk superconducting nano samples exhibit smaller grain size than the undoped Y-123 sample. Differences in size may be caused by

Table 1 Some structural values of Zn-doped Y-123 nano bulk materials

Samples	a (Å)	b (Å)	c (Å)	Grain size (nm)	T_c^{onset} (K)
Zn0.0	3.81	3.89	11.65	30.56	89
Zn0.01	3.81	3.86	11.61	30.18	84
Zn0.03	3.81	3.86	11.60	29.77	79
Zn0.10	3.82	3.84	11.57	28.11	61
Zn0.30	3.83	3.84	11.57	28.23	60

ionic radius differences between Cu^{2+} (0.73 Å) and the Zn^{2+} (0.74Å) doping elements.

3.2 Electrical Resistivity Measurements of Superconducting Nanoparticles

The temperature dependence of normalized resistivity (ρ-T) of undoped and Zn-doped samples produced in this study is given in Fig. 2. It is observed that all the samples show metallic behavior above the T_c^{onset} temperature. The T_c^{onset} is 89 K for the undoped sample, and the T_c^{onset} value decreases monotically with Zn doping. The T_c^{offset} value of the undoped sample is 84 K, and it decreases monotically with Zn doping (Table 1).

The grain size of the Y-123 sample reduces with the Zn doping. The resistivity increases with Zn doping compared with undoped Y-123 sample. Because the grain sizes decrease with Zn, the number of contacts between grains increases the resistivity [16–18].

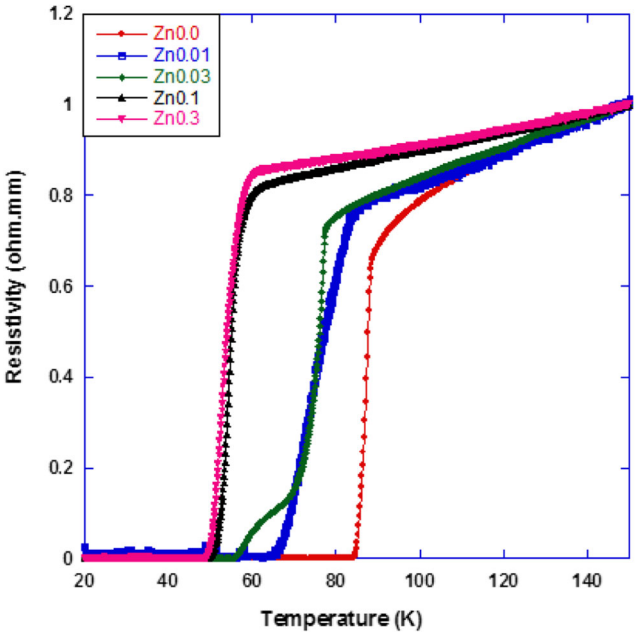

Fig. 2 Normalized resistivity as a function of temperature curves for the samples

3.3 Vickers Microhardness Measurements of Superconducting Nanoparticles

Microhardness tests are developed to measure the hardness of materials. Among these tests, the Vickers microhardness test can be used for all materials and has one of the broadest scales.

Hardness is determined when force is applied by an indenter to the surface area. Vickers microhardness value is calculated by (1).

$$H_{vV} = 1854.4(F/d^2)\ (\text{GPa}) \quad (1)$$

where H_V is the Vickers microhardness in gigapascalsGPa, F is the applied load in newtons, and d is the diagonal length of the indentation in micrometers. In order to investigate the effect of doping rate on the mechanical properties, Vickers microhardness measurements are performed on the sample surfaces at the room temperature. The applied load is changed in the range 0.245–2.940 N for 10 s. Microhardness values are determined with an average of seven readings at different parts of the sample surfaces, making sure that the indentations do not overlap.

The change of the load-dependent microhardness values as a function of the test loads is shown in Fig. 3 in detail. It can be seen from figure that the microhardness values decrease with increased Zn doping in the Y-123 Y123 structure. In addition, microhardness values reach a plateau (saturation region) at around 1.5 N for all the samples. The hardness value of the sample observed reverse indentation size effect (RISE) behavior depends on the applied load [19–21]. That is, the hardness increases with

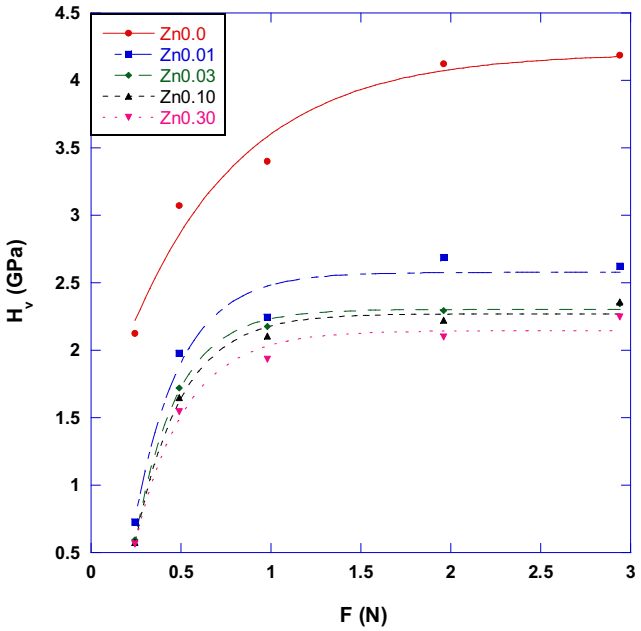

Fig. 3 The variations of microhardness with load for the samples

the applied load. The hardness value of the sample observed to have RISE behavior depends on the applied load. It shows that the indenter size is associated with applied load. This non-linear case is named as reverse indentation size effect in the literature [22–25]. Smaller indentation load shows a smaller hardness value. In addition, the optical trace photos of the indentations for each sample under 2.940 N load are shown in Fig. 4.

3.3.1 Description of Mechanical Parameters

The modulus of elasticity (E) is a measure of elastic deformation of the material under force. In some sources, it is also referred to as Young's modulus and calculated as described below. Materials become more rigid with increasing the E. In order words, material shows less deformation with strain. When elasticity modulus is small, the material acts more flexible/elastic.

$$E = 81.9635\, H_{\mathrm{V}} \tag{2}$$

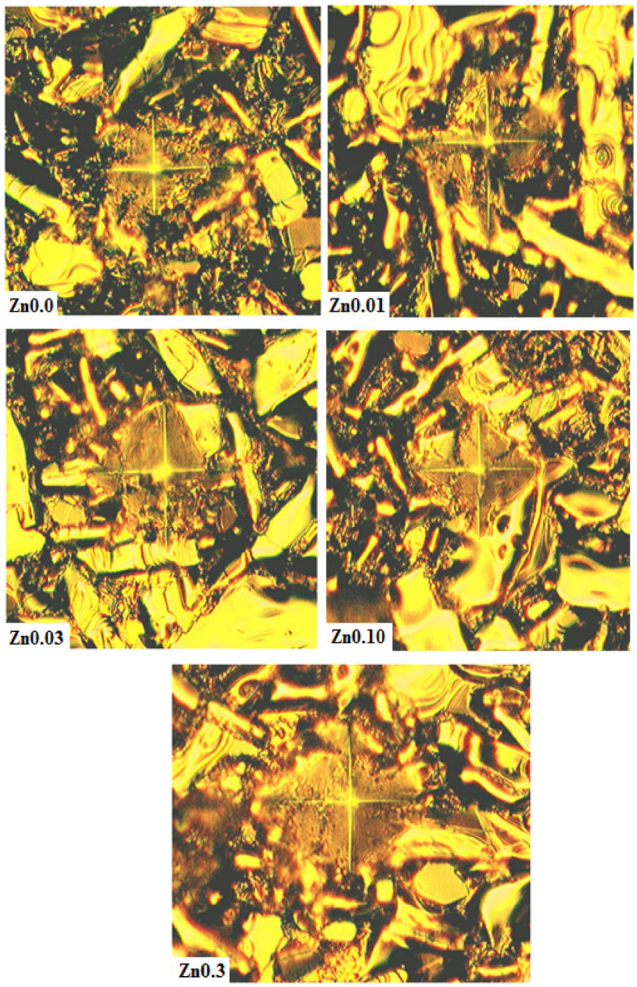

Fig. 4 The optical trace photos under 2.940 N load for all the samples

Brittleness (B_i) is the tendency of a material has undergone very little fracture or has no deformation that is predetermined to fracture in technical using. It means that material does not have the ability to plastic deformation. B_i is the opposite ductility (D). Ductility is the ability of a material to permanent deformation.

$$B_i = H_{\mathrm{vV}}/K_{\mathrm{IC}} \tag{3}$$

$$D = 1/B_i \tag{4}$$

Toughness of the material is a maximum amount of energy absorbed before fracture. At the same time, it is described as plastic deformation capability of the material. Because elastic and plastic deformation allows for absorption of a majority of energy by the material, toughness can be small in brittle materials. In materials science, fracture toughness is a property that defines the ability of the material which contains cracks formed by fracture and is one of the important features of any material in many design applications. Linear elastic fracture toughness of a material is determined by the formation of a crack that begins to grow in the material. It is shown as fracture toughness (K_{IC})

$$K_{\mathrm{IC}} = \sqrt{2E\gamma} \tag{5}$$

Yield strength (Y) represents the transition point from elastic deformation to plastic deformation.

$$Y \approx H_{\mathrm{V}}/3 \tag{6}$$

The load-dependent values of E, Y, K_{IC}, B_i, and D are summarized in Table 2. It is visible from the table that these values decrease with increasing the Zn content and increase with the applied test load. We can say from table that E, Y, K_{IC}, B_i, and D values decrease because these parameters are in relation to the hardness. K_{IC}, B_i, and D values are negative. It confirms that the character of the displacement of these materials is in the form of the RISE behavior and the plastic deformations occur in these samples which show the RISE behavior.

Nowadays, it seems that technological device, equipment, vehicles, machine, and constructions which are manufactured and used for various industrial purposes are manufactured from materials such as metal, ceramic, glass, plastic, paper, and composites that have different properties. The selection of the most qualified, the most durable, and the most economic materials is very important due to the service conditions, the applied load type and value, and the place of use of each product by design engineers. The electrical, optical, thermal, and corrosion properties of materials must be known very well for selection of material. At this point, it is quite important to determine the mechanical properties of materials.

Table 2 The calculated load-dependent H_v, E, Y, B_i, and D for the samples

Samples	F (N)	H_v (GPa)	Plateau region (GPa)	E (GPa)	Y (GPa)	B_i ($m^{1/2}$)	D ($m^{-1/2}$)	K_{IC} ($Pa/m^{1/2}$)
Zn0.0	0.245	2.126	3.401–4.186	174.27	0.708	−0.717	−1.394	−2.963
	0.490	3.073		251.93	1.024	−0.862	−1.160	−3.563
	0.980	3.401		278.78	1.133	−0.907	−1.102	−3.748
	1.960	4.121		337.84	1.373	−0.998	−1.002	−4.126
	2.940	4.186		343.11	1.395	−1.006	−0.994	−4.158
Zn0.01	0.245	0.728	2.245–2.621	59.72	0.242	−0.390	−2.563	−1.867
	0.490	1.979		162.23	0.659	−0.643	−1.555	−3.078
	0.980	2.245		184.08	0.748	−0.684	−1.459	−3.278
	1.960	2.687		220.30	0.895	−0.749	−1.334	−3.586
	2.940	2.621		214.87	0.873	−0.740	−1.351	−3.542
Zn0.03	0.245	0.594	2.174–2.346	48.737	0.198	−0.369	−2.707	−1.610
	0.490	1.719		140.96	0.573	−0.628	−1.592	−2.738
	0.980	2.174		178.21	0.724	−0.706	−1.416	−3.079
	1.960	2.295		188.18	0.765	−0.725	−1.378	−3.164
	2.940	2.346		192.29	0.782	−0.733	−1.363	−3.198
Zn0.10	0.245	0.576	2.105–2.360	47.21	0.192	−0.346	−2.880	−1.663
	0.490	1.651		135.32	0.550	−0.586	−1.705	−2.816
	0.980	2.105		172.54	0.701	−0.662	−1.510	−3.179
	1.960	2.224		182.28	0.741	−0.680	−1.469	−3.268
	2.940	2.360		193.43	0.786	−0.700	−1.426	−3.366
Zn0.30	0.245	0.564	1.933–2.248	46.24	0.188	−0.337	−2.962	−1.671
	0.490	1.545		126.64	0.515	−0.558	−1.789	−2.765
	0.980	1.933		158.48	0.644	−0.624	−1.600	−3.093
	1.960	2.098		172.00	0.699	−0.651	−1.535	−3.223
	2.940	2.248		184.27	0.749	−0.673	−1.483	−3.336

In this study, microhardness values of Y-123 superconductors decrease with increasing the Zn doping. The material produced must be assessed according to the area used in technology. If a superconducting cable is to be produced, a material that has a lower hardness (more elastic) should be selected.

4 Conclusion

In this study, the superconducting $YBa_2Cu_{3-x}Zn_xO_7$ (Y-123) bulk materials have been synthesized by using the sol-gel method. XRD, R-T, and Vickers microhardness measurements were carried out for structural, mechanical, and superconducting properties of prepared samples. According to XRD and R-T measurements, an orthorhombic structure has not changed with Zn doping and all samples exhibit superconducting property. T_c^{onset} is 89 K for undoped Y-123 sample, and the T_c^{onset} value decreases monotically with Zn addition. All samples show metallic behavior above T_c^{onset} temperature. In addition to these analyses, according to Vickers microhardness, undoped and Zn-doped Y-123 samples have RISE behavior.

Funding Information This study was supported by the Kastamonu University Scientific Research Projects Coordination Department under the Grant No. KÜ-BAP01/2016-21. Besides I would like to thank the Kastamonu University Research and Application Center for the supports.

References

1. Wu, K.M., Ashburn, J.R., Torng, C.: Superconductivity at 93 K in a new mixed-phase YBCO compound system at ambient pressure. Phys. Rev. Lett. **58**, 908–910 (1987)
2. Jorgensen, J.D., Beno, M.A., Hinks, D.G.: Oxygen ordering and the orthorhombic to tetragonal phase transition in YBCO. Phys. Rev. B **36**, 3608–3616 (1987)
3. Cogollo, R.P., Marino, A.C., Sanchez, H.M.: Transport properties of YBCO superconducting films at different oxygen concentration. IEEE Trans. Appl. Supercond. **13**, 2789–2791 (2003)
4. Gonzales, J.K.: Coated conductors and chemical solution growth of YBCO Universitat Autonoma de Barcelona Thesis of the PhD (2005)
5. Koelle, D.: High transition temperature superconducting quantum interference devices: basic concepts, fabrication and applications. J. Electroceram. **3**, 195–212 (1999)
6. Şahin, O., Uzun, O., Kölemen, U., Uçar, N.: Dynamic hardness and reduced modulus determination on the (001) face of B-sn single crystals by a depth sensing indentation technique. J. Phys. Condens. Matter. **306001**, 19 (2007)

7. Sangwal, K., Surowska, B., Blaziak, P.: Analysis of the indentatıon size effect in the microhardness measurement of some cobalt-based alloys. Mater. Chem. Phys. **77**, 511 (2002)
8. Graaf, D.D., Braciszewicz, M., Hintzen, H.T., Sopicka-Lizer, M., De With, G.: The influence of the composition on (the load-dependence of) the microhardness of Y-;Si-;Al-;O-;N glasses as measured by Vickers indentation. J. Mater. Sci. **39**, 2145 (2004)
9. Lopesa, E.S.N., Cremascoa, A., Afonsob, C.R.M., Caram, R.: Effects of double aging heat treatment on the microstructure, Vickers hardness and elastic modulus of Ti–Nb alloys. Mater. Charact. **62**, 673–680 (2011)
10. Tosun, M., Ataoglu, S., Arda, L., Ozturk, O., Asikuzun, E., Akcan, D., Cakiroglu, O.: Structural and mechanical properties of ZnMgO nanoparticles. Mater. Sci. Eng.: A **590**, 416–422 (2014)
11. Ozturk, O., Asikuzun, E., Yildirim, G.: The role of Lu doping on microstructural and superconducting properties of $Bi_2Sr_2CaLu_xCu_2O_y$ superconducting system. J. Mat. Sci.: in Elect. **24**, 1274–1281 (2013)
12. Arda, L., Ozturk, O., Asikuzun, E., Ataoglu, S.: Structural and mechanical properties of transitions metals doped ZnMgO nanoparticles. Powder Technol. **235**, 479–484 (2013)
13. Asikuzun, E., Ozturk, O., Arda, L., Akcan, D., Senol, S.D., Terzioglu, C.: Preparation, structural and micromechanical properties of (Al/Mg) co-doped ZnO nanoparticles by sol–gel process. J. Mat. Sci.: in Elect. **26**, 8147–8159 (2015)
14. Gotor, F.J., Odier, P., Gervais, M., Choisnet, J., Monod, P.: Synthesis of $YBa_2Cu_30_{7-x}$ by sol-gel route Formation of YBaCuO oxycarbonate intermediate. Phys. C **218**, 429–436 (1993)
15. Alikhanzadeh Arani, S., Salavati Niasari, M.: Synthesis and characterization of high-temperature ceramic YBCO nanostructures prepared from a novel precursor. J. Nanostructure **1**, 62–68 (2012)
16. Aksan, M.A., Yakinci, M.E.: Thermal and superconducting properties of glass–ceramic ht_c BiSrCa(CuPr)O system. J. Mater. Process. Technol. **196**, 365–372 (2008)
17. Terzioglu, C.: EDXRF measurements on gold diffusion-doped $Bi_{1.8}Pb_{0.35}Sr_{1.9}Ca_{2.1}Cu_3O_y$. Physica B **403**, 3320–3325 (2008)
18. Ozturk, O., Asikuzun, E., Kaya, S., Soylu, N., Erdem, M.: The effect of Ar ambient pressure and annealing duration on the microstructure, superconducting properties and activation energies of MgB_2 superconductors. J. Supercond. Novel Magn. **30**, 1161–1169 (2017)
19. Arda, L., Ozturk, O., Asikuzun, E., Ataoglu, S., Ataoglu, S.: Structural and mechanical properties of transition metals doped ZnMgO nanoparticles. Powder Technol. **35**, 479–484 (2013)
20. Kölemen, U., Uzun, O., Ylmazlar, M., Güçlü, N., Yanmaz, E.: Hardness and microstructural analysis of $Bi_{1.6}Pb_{0.4}Sr_2Ca_{2-x}Sm_xCu_3O_y$ polycrystalline superconductors. J. Alloys Compd. **415**, 300–306 (2006)
21. Sahin, O., Uzun, O., Sopicka-Lizer, M., Gocmez, H., Kölemen, U.: Dynamic hardness and elastic modulus calculation of porous sialON ceramics using depth-sensing indentation technique. J. Eur. Ceram. Soc. **28**, 1235–1242 (2008)
22. Koralay, H., Hicyilmaz, O., Cavdar, S., Asikuzun, E., Tasci, A.T., Ozturk, O.: Effect of Zn content on microstructure and mechanical performance in $Bi_{1.8}Sr_2Ca_2Cu_{3.22-x}Zn_xO_{10+}$ glass ceramic. J. Mater. Sci. Mater. Electron. **25**, 3116–3126 (2014)
23. Gong, J., Wu, J., Guan, Z.: Examination of the indentation size effect in low-load Vickers hardness testing of ceramics. J. Eur. Ceram. Soc. **19**, 2625–2631 (1999)
24. Elmustafa, A.A., Stone, D.S.: Nanoindentation and the indentation size effect: kinetics of deformation and strain gradient plasticity. J. Mech. Phys. Solid **51**, 357–381 (2003)
25. Safran, S., Ozturk, H., Bulut, F., Ozturk, O.: The influence of re-pelletization and heat treatment on physical, superconducting, magnetic and micro-mechanical properties of bulk BSCCO samples prepared by ammonium nitrate precipitation method. Ceram. Int. **43**, 15586–15592 (2017)